Stress corrosion cracking and surface oxidation properties of Ni-base welding alloys exposed to PWR primary water

Yun Soo Lim*, Dong Jin Kim, Sung Woo Kim, Seong Sik Hwang, Hong Pyo Kim
Korea Atomic Energy Research Institute/Nuclear Materials Research Division
1045 Daedeok-daero, Yuseong-gu, Daejeon, 305-353, Korea
**Corresponding author: yslim@kaeri.re.kr*

1. Introduction

In-service cracking at the penetration nozzles and surrounding welds of the reactor pressure vessel head (RPVH) of a pressurized water reactor (PWR) has been found after long-term operation. Alloy 182 is widely used as a filler or butter material for dissimilar metal welds to join Alloy 600 with stainless steel and/or low alloy steel. It is now well established that Alloy 600 and Alloy 182 are susceptible to stress corrosion cracking (SCC) in primary water environments, which is known as primary water SCC (PWSCC). The cracking of Alloy 600 and Alloy 182 in most cases was identified as intergranular SCC (IGSCC) [1,2]. Because cracks initiate and propagate along the grain boundaries on the surface, the susceptibility of these materials to PWSCC is influenced by the surface properties, grain boundary chemistry and structure, and the degree of the precipitation of intergranular (IG) Cr carbides.

Alloy 690, another Ni-based alloy, has been replacing Alloy 600, and Alloy 152 filler metal has also been used to join Alloy 690 components instead of Alloy 182. Alloy 690 and Alloy 152 are known to be more resistant to PWSCC than Alloy 600 and Alloy 182 owing to their higher Cr contents. A heterogeneous microstructure is generated in the weld metal by anisotropic dendritic growth and the local microsegregation of the alloying constituents during the welding process. Therefore, the PWSCC resistance of a weld metal can differ somewhat depending on the orientation of crack propagation.

The aim of the present study is to compare the PWSCC resistances of Alloy 182 and Alloy 152 welds by measuring the crack growth rate (CGR) using a compact tension (CT) specimen in a simulated PWR primary water condition. Surface oxidation tests are also conducted under identical experimental conditions to obtain clues with which to understand the cracking phenomena. The cracking and surface oxidation characteristics are also examined using microscopic equipment. Finally, the different characteristics of PWSCC of the test welds are discussed in terms of cracking and surface oxidation behavior.

2. Methods and Results

2.1 Materials Preparation and PWSCC Test

A mill annealed Alloy 600 round bar was used to fabricate an Alloy 600/182 weld. The round bar was cut in half, and an 80 mm wide × 40 mm deep upside-down trapezoidal groove was made in the center of the bar. The groove was filled with the Alloy 182 filler metal by multi-pass submerged arc welding. A similar process was used to create an Alloy 690/152 weld. The 1/2T CT specimens for PWSCC test were taken from the welded parts such that the cracking planes were parallel to the growth direction of the primary dendrites. Fig. 1(a) and (b) show the geometries of weldment (in mm) and the regions where CT specimens were taken from the Alloy/182 weld and the Alloy 690/152 weld, respectively.

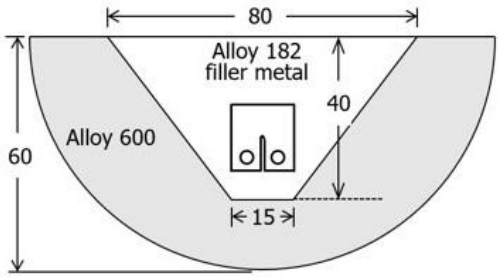

(a)

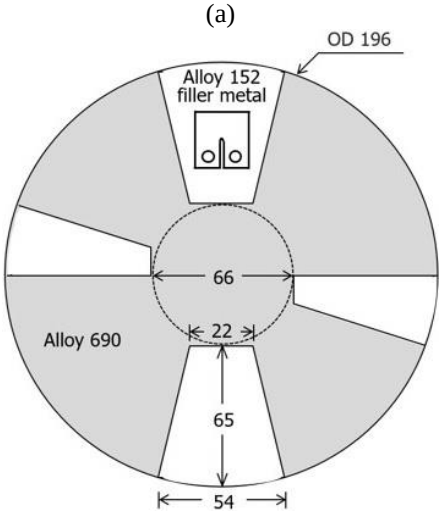

(b)

Fig. 1. The geometries of weldment and the region where a CT specimen was taken from (a) the Alloy/182 weld and (b) the Alloy 690/152 weld, respectively

Before the PWSCC test, the two CT specimens were pre-cracked by fatigue at lengths of 2 mm and 1.8 mm at room temperature in air, respectively. The test was conducted under simulated PWR primary water environmental conditions, that is, 1200 ppm B (weight)

as H_3BO_3 and 2 ppm Li (weight) as LiOH in pure water at 325 ℃, a dissolved oxygen content below 5 ppb, a hydrogen partial pressure of 98.6 kPa, and an internal pressure of 15.9 MPa. The variation in the crack length of the specimen during the test was estimated using the direct current potential drop (DCPD) method [4], and the stress intensity factor at the crack tip was maintained at 30 MPa√m throughout the test. A surface oxidation test was conducted in the same environments for the PWSCC test for 3,600 hours.

2.2 Microscopic Examinations

After the PWSCC test, the specimen for CGR test was fractured to examine the fracture surface. The specimens for the optical microscopy (OM) and scanning electron microscopy (SEM) were prepared by chemical etching in a solution of 2 vol% bromine + 98 vol% methanol. The TEM specimens containing PWSCC crack tips or surface oxidation layers were prepared through focused ion beam (FIB) milling using a dual beam Hitachi FIB-2100 system with Ga+ incident beam energy of 30 kV and current of 1–5 nA.

An SEM examination was conducted using a JEOL 5200 (operating voltage 25 kV) and a JEOL 6300 (operating voltage 20 kV). A scanning TEM (STEM) analysis was carried out with a JEOL JEM-2100F (operating voltage 200 kV) equipped with an Oxford Instruments X-max80T Silicon Drift Detector (SDD) and an AZTEC analysis system (Ver. 3.1b). Energy dispersive spectroscopy (EDS) spectrum imaging was conducted with a dwell time per pixel of 43.9 ms, energy per channel of 20 eV, and a process time of 16 μs. The modified Cliff-Lorimer method was used for the quantification of the EDS point analysis. The peaks of the Cr L_α line (0.50 KeV) and the oxygen K line (0.52 KeV) are in close proximity in the EDS spectrum; there is intrinsically some overlap between these two peaks. Therefore, deconvolution of the overlapping spectral peaks was carried out for a clear determination of the oxygen and Cr constituent peaks.

2.3 Cracking Properties

The average CGR of Alloy 182 was measured to be 1.0×10^{-7} mm/s at K = 30 MPa√m. This value is located within the range of experimental CGR data obtained under environment and stress conditions identical to those used here [4], indicating that the susceptibility to PWSCC of the Alloy 182 under test is relatively high. While the CGR value of Alloy 152 was 2.4×10^{-9} mm/s at K = 30 MPa√m. This result confirms that the resistance to PWSCC of Alloy 152 is much higher than that of Alloy 182. The main reason for the high PWSCC resistance of Alloy 152 may be the high Cr content.

The crack propagation outcome in the Alloy 182 weld is shown in Fig. 2(a). As shown in the figure, the crack propagated along a grain boundary, which means that the cracking mode is clearly IGSCC. The fractured surface morphology of Alloy 182 after the PWSCC test was clearly shown to be IG, and the grain shapes of the weld metal were clearly visible, providing evidence of IGSCC.

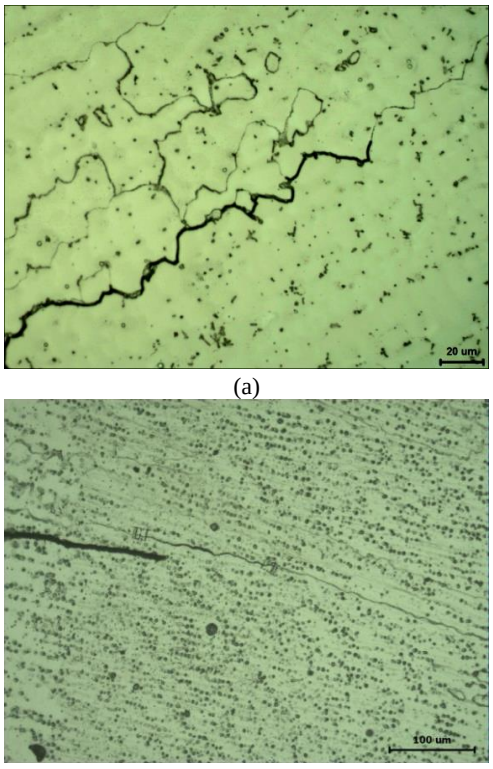

(a)

(b)

Fig. 2. OM images of (a) Alloy 182 and (b) Alloy 152 welds showing cracking properties.

Given that the CGR of Alloy 152 was very low, cracks propagated only for short distances. Fig. 2(b) shows the overall morphology of the crack propagation outcome in the Alloy 152 weld. Unlike that in Alloy 182, the primary crack did not necessarily propagated along the grain boundaries. Rather, it advanced in a mixed (IG+transgranular) mode. Contrary to the primary crack, many secondary cracks propagated along the grain boundary. Most of the PWSCC area in the fractured surface morphology showed transgranular fracturing, though there were also some IG cracking areas. These results clearly demonstrate that the cracks in the Alloy 152 weld propagate in a mixed mode. This behavior is quite different from that of Alloy 182, in which most of the cracks propagate along grain boundaries.

2.4 Surface Oxidation Behavior

When oxygen diffuses into an alloy, two types of alterations arise. Cr is selectively oxidized by oxygen diffusion on the surface to form a Cr oxide, which is most likely Cr_2O_3. These surface Cr oxides serves as the main protective layer. The grain boundary is also

affected by oxygen diffusion, and Cr oxides form at the grain boundary as well, from which Cr depletion and Ni enrichment occur around the Cr oxides ahead of the SCC crack tips [1]. The grain boundary can then become brittle, readily leading to IG cracking.

Fig. 3 was obtained from the Alloy 182 weld metal, and it shows a STEM image and EDS spectrum images of O, Cr, Ni, Fe and Mn obtained using the Kα1 lines around the surface. A grain boundary is visible in the STEM image. In the O spectrum image, a surface inner layer with a thin continuous Cr-rich oxide layer appears to emerge. The most intriguing feature in Fig. 3 is that oxygen diffused down along the grain boundary (dotted circle in the O spectrum image), causing the grain boundary to be oxidized. On the oxidized grain boundaries, Cr was enriched and Cr oxides formed (dotted rectangles in the O and Cr spectrum images). However, Ni and Mn were depleted in the oxidized grain boundary (Ni and Mn spectrum images) compared to the average concentration of the matrix. All of these results are in good agreement with those of Alloy 600 obtained under similar test conditions [1,5].

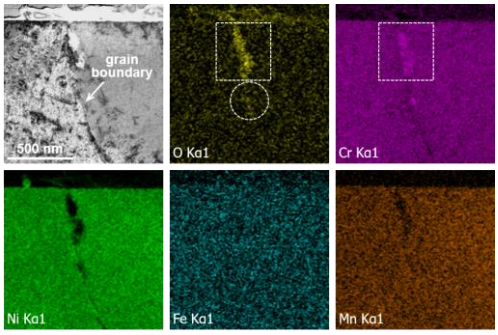

Fig. 3. STEM image, and EDS spectrum images of O, Cr, Ni, Fe and Mn taken from the Alloy 182 weld.

Fig. 4 was obtained from the Alloy 152 weld metal, showing a STEM image and EDS spectrum images of O, Cr, Ni, Fe and Mn obtained using the Kα1 lines around the surface. The surface oxidation layer was much thicker than that of the Alloy 182 weld, as confirmed from the O spectrum image in Fig. 3. The most noticeable difference is that there is no oxygen diffusion along the grain boundary (dotted circle in the O spectrum image). Other intriguing findings are that Cr was depleted (dotted circle in the Cr spectrum image) and Ni was enriched (dotted circle in the Ni spectrum image), in direct contrast to the Alloy 182 weld. From these results, it can be confirmed that the surface oxidation phenomena of the Alloy 152 weld was quite different from those of the Alloy 182 weld. The main reason for this difference is thought to be the different chemical compositions, especially the different Cr contents in these two alloys. These surface oxidation phenomena are similar to those of Alloy 690 obtained in a simulated PWR environment [6].

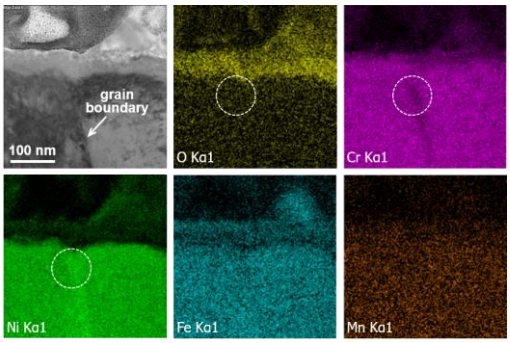

Fig. 4. STEM image, and EDS spectrum images of O, Cr, Ni, Fe and Mn taken from the Alloy 152 weld

The major finding in the current study is that there was a noticeable difference in the IG oxidation behavior between Alloy 182 and Alloy 152. Oxygen diffused into the grain boundary in Alloy 182 (Fig. 3), but IG oxidation did not occur in the Alloy 152 weld (Fig. 4). When IG oxidation occurs by pre-exposure to primary water, embrittlement of the grain boundaries is known to take place, leading to IG ruptures during SCC tests. Fujii et al. [7] showed that an IG fracture readily occurred even under a small amount of applied stress when the grain boundaries were attacked by a pre-oxidization treatment.

Alloy 152 is known to be more resistant to PWSCC than Alloy 182 due to its higher Cr content. The lack of IG oxidation in the Alloy 152 weld can partly explain why it has higher resistance to PWSCC, compared to that of the Alloy 182 weld, because crack propagation can be very rapid when IG cracking occurs. It can also demonstrate why Alloy 152 shows mixed cracking, instead of IG cracking such as Alloy 600 and Alloy 182. The different IG oxidation behavior in the Alloy 182 and 152 welds appears to lead to the different cracking resistance, and the different cracking modes as well.

3. Conclusions

From the CGR tests, it was confirmed that the resistance to PWSCC of Alloy 152 weld was much higher that of Alloy 182 weld. Oxygen diffused down along the grain boundary in Alloy 182 from the outer environment, causing IG oxidation. As a result of the oxygen diffusion, Cr oxide formed in the oxidized grain boundary. These changes in the grain boundary can significantly lower the strength of that grain boundary and therefore increase the level of sensitivity to PWSCC when stress is applied. IG oxidation due to oxygen diffusion and the resultant embrittlement of the grain boundaries are believed to be significant factors related to the occurrence of IG cracking in Alloy 182. Oxygen was, however, not detected in the grain boundary of the Alloy 152 weld. This finding implies that oxygen diffusion along the grain boundaries is significantly suppressed in Alloy 152 welds. Consequently, the IG

oxidation behavior was found to be closely correlated with the known SCC properties of the two alloys.

REFERENCES

[1] Y.S. Lim, H.P. Kim, and S.S. Hwang, Microstructural characterization of intergranular stress corrosion cracking of alloy 600 in PWR primary water environment, J. Nucl. Mater., Vol.440, p. 46, 2013.
[2] L.E. Thomas, M.J. Olszta, B.R. Johnson, and S.M. Bruemmer, Microstructural characterization of primary water stress-corrosion cracks in Alloy 182 welds from PWR components and laboratory tests, Proceedings of the 14th Int. Conf. on Environmental Degradation of Materials in Nuclear Power Systems-Water Reactor, p. 409, 2009, Virginia Beach, VA.
[3] M.A. Hicks and A.C. Pickard, A comparison of theoretical and experimental methods of calibrating the electrical potential drop technique for crack length determination, Int. J. Fract., Vol.20, p.91, 1982.
[4] G.A. White, J. Hickling, and L.K. Mathews, Crack Growth Rates for Evaluating PWSCC of Thick-Wall Alloy 600 Material, Proceedings of the 11th Int'l Conf. on Environmental Degradation of Materials in Nuclear Power Systems–Water Reactor, p.166, 2003, Stevenson, WA.
[5] Y.S. Lim, S.W. Kim, S.S. Hwang, H.P. Kim, and C. Jang, Intergranular oxidation of Ni-based Alloy 600 in a simulated PWR primary water environment, Corrosion Science, Vol.108, p. 125, 2016.
[6] S.Y. Persaud, S. Ramamurthy, and R.C. Newman, Internal oxidation of alloy 690 in hydrogenated steam, Corrosion Science, Vol.90, p. 606, 2015.
[7] K. Fujii, T. Miura, H. Nishioka, and K. Fukuya, Degradation of grain boundary strength by oxidation in alloy 600, Proceedings of the 15th Int. Conf. on Environmental Degradation of Materials in Nuclear Power Systems-Water Reactor, p. 1447, 2011, Colorado Springs, Colorado.